



OPEN

## A diagnostic model for differentiating tuberculous spondylitis from pyogenic spondylitis: a retrospective case–control study

Yu Xi Liu, Fei Lei, Li Peng Zheng, Hao Yuan, Qing Zhong Zhou & Da Xiong Feng

The purpose of this study was to describe and compare the clinical data, laboratory examination and imaging examination of tuberculous spondylitis (TS) and pyogenic spondylitis (PS), and to provide ideas for diagnosis and treatment intervention. The patients with TS or PS diagnosed by pathology who first occurred in our hospital from September 2018 to November 2021 were studied retrospectively. The clinical data, laboratory results and imaging findings of the two groups were analyzed and compared. The diagnostic model was constructed by binary logistic regression. In addition, an external validation group was used to verify the effectiveness of the diagnostic model. A total of 112 patients were included, including 65 cases of TS with an average age of  $49 \pm 15$  years, 47 cases of PS with an average of  $56 \pm 10$  years. The PS group had a significantly older age than the TS group ( $P = 0.005$ ). In laboratory examination, there were significant differences in WBC, neutrophil (N), lymphocyte (L), ESR, CRP, fibrinogen (FIB), serum albumin (A) and sodium (Na). The difference was also statistically significant in the comparison of imaging examinations at epidural abscesses, paravertebral abscesses, spinal cord compression, involvement of cervical, lumbar and thoracic vertebrae. This study constructed a diagnostic model, which was  $Y$  (value of  $TS > 0.5$ , value of  $PS < 0.5$ ) =  $1.251 * X1$  (thoracic vertebrae involved = 1, thoracic vertebrae uninvolved = 0) +  $2.021 * X2$  (paravertebral abscesses = 1, no paravertebral abscess = 0) +  $2.432 * X3$  (spinal cord compression = 1, no spinal cord compression = 0) +  $0.18 * X4$  (value of serum A) –  $4.209 * X5$  (cervical vertebrae involved = 1, cervical vertebrae uninvolved = 0) –  $0.02 * X6$  (value of ESR) –  $0.806 * X7$  (value of FIB) – 3.36. Furthermore, the diagnostic model was validated using an external validation group, indicating a certain value in diagnosing TS and PS. This study puts forward a diagnostic model for the diagnosis of TS and PS in spinal infection for the first time, which has potential guiding value in the diagnosis of them and provides a certain reference for clinical work.

Spinal infection may involve the vertebrae, the intervertebral discs, and the adjacent intraspinal and paraspinal soft tissues<sup>1</sup>. During the development of the disease, the formation of abscesses or edemas can destroy vertebrae or cause neurologic disorders. Recently, the incidence of spondylitis has increased due to longer life expectancy of patients with chronic debilitating diseases<sup>2–4</sup>.

Tuberculous spondylitis (TS) results from dissemination of the tuberculous bacilli from a distant active source or as a result of latent reactivation, and pyogenic spondylodiscitis (PS) refers to infectious spondylodiscitis caused by ordinary bacteria. Differentiation between TS and PS is essential for deciding on the appropriate therapeutic regimen. Although bacterial culture is considered the gold standard for diagnosing infectious diseases, it may have low positivity rates due to unreasonable antibiotic use before tissue sampling or difficulty in culturing the causative agent<sup>3,6</sup>. Meanwhile, spinal infection symptoms often have a non-specific and insidious onset, and identifying the etiological agent can be elusive in about a third of spinal infection cases<sup>7</sup>. Although various diagnostic techniques such as computed tomography (CT), magnetic resonance imaging (MRI) and positron emission tomography have been used in clinical practice, there are still limitations<sup>8–10</sup>. CT has a good

Department of Orthopaedics, The Affiliated Hospital of Southwest Medical University, No. 25 Taiping Street, Lu Zhou City, China. email: 19382402617@163.com

sensitivity in evaluating bony changes, but it may not be sufficient for some patients with TS who lack typical sequestra and pathological calcifications<sup>11</sup>. In contrast, MRI with gadolinium enhancement is widely recognized as the most reliable method for diagnosing spinal infection. However, while there are features that can suggest either TS or PS, there is a significant overlap between the two. As for positron emission tomography CT with F-18 fluorodeoxyglucose (<sup>18</sup>FDG PET-CT), it can only suggest an infectious disease and has limited value in differentiating between TS and PS<sup>12,13</sup>.

The aim of this study was to describe and compare the clinical data, laboratory examination and imaging examination of TS and PS, and to provide a diagnostic model for diagnosis and treatment intervention.

## Materials and methods

The current study conformed to the principles drafted in the Helsinki declaration and was approved by the medical ethical committee of the Affiliated Hospital of Southwest Medical University (approval number: KY2022262). The need for consent was waived by the ethical committee of the Affiliated Hospital of Southwest Medical University due to the retrospective nature of this study. The study evaluated the clinical, laboratory and imaging data of 65 patients with TS (the TS group) and 47 patients with PS (the PS group) in a single institution from September 2018 to November 2021. And 25 TS patients (the EV-TS group) and 21 PS patients (the EV-PS group) who had continuous medical visits from December 2021 to April 2023 were used as an external validation group to verify the diagnostic model. All patients diagnosed by pathology (Fig. 1). The inclusion criteria included the following: age  $\geq$  18 years old; admitted to hospital for the first time because of spinal infection; cervical, thoracic or lumbosacral vertebrae infection. The exclusion criteria included the following: infection caused by invasive examination or surgery of the spine; previous surgical history of spinal infection; complication with tumor or autoimmune disease; complication with bone or joint infection in other parts; and incomplete medical record or radiological examination.

Clinical information including sex, age and course of disease were retrieved from the electronic medical record system for patients. Laboratory examination: fasting venous blood was collected at 6:00 a.m. the day after admission to collect blood infection markers, function of blood coagulation, kidney function tests, liver function tests and serum electrolytes. The blood infection markers included leukocyte (WBC), neutrophil (N), eosinophil (E), basophil (B), lymphocyte (L), monocyte (M), erythrocyte sedimentation rate (ESR) and C-reactive protein (CRP). The function of blood coagulation included platelet (PLT), prothrombin time (PT), activated partial thromboplastin time (APTT), prothrombin time (TT) and fibrinogen (FIB). The kidney function tests included creatinine (Cr) and glomerular filtration rate (GFR). The liver function tests included albumin (A), globulin (G),

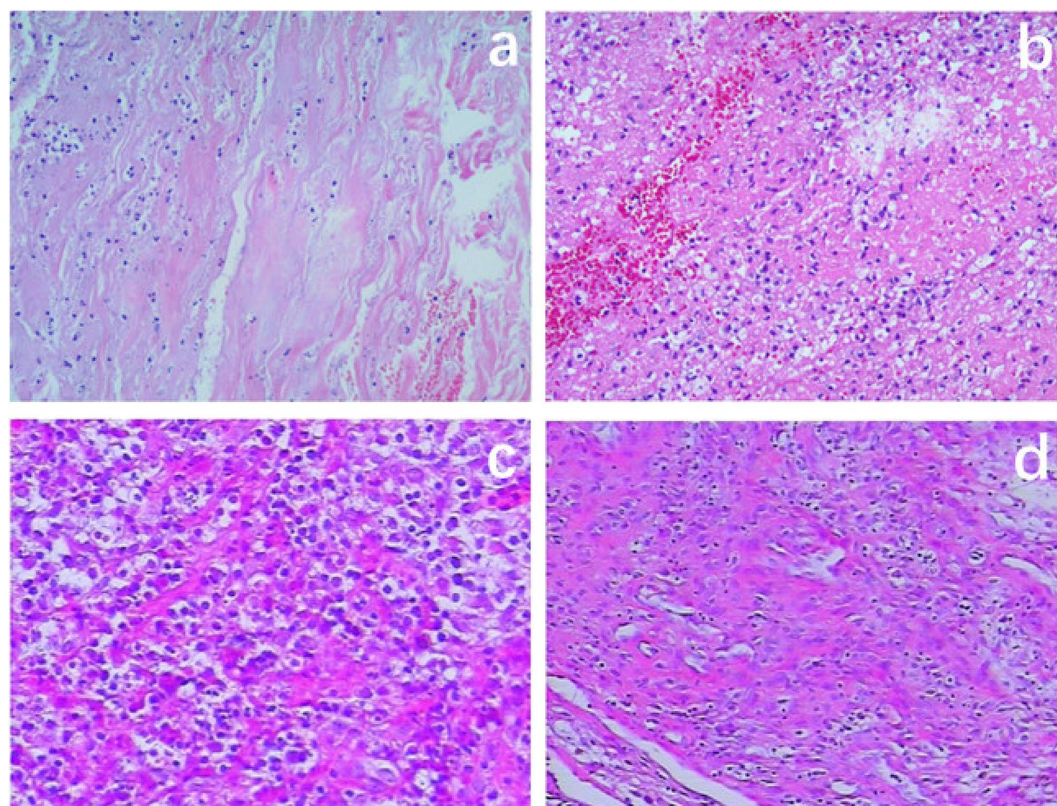


**Figure 1.** Pathological specimens of tuberculous spondylitis and pyogenic spondylodiscitis. (a) and (b) Pathological specimens of tuberculous spondylitis. Visible granulomatous inflammation and caseous necrosis. (c) and (d) Pathological specimens of pyogenic spondylodiscitis. Visible chronic suppurative inflammation with extensive proliferation of inflammatory granulation tissue.

alanine transaminase (ALT) and aspartate transaminase (AST). The serum electrolytes included potassium (K), sodium (Na), calcium (Ca) and chlorine (Cl).

Imaging assessment on admission included computed tomography scans (CT) and magnetic resonance imaging (MRI). The following lesions were sought on CT images: (1) disc space narrowing; (2) bone destruction of vertebral body; (3) destruction of pedicle bone. The following lesions were sought on MRI: (1) vertebral involvement (single-segment, multiple-segments, cervical, thoracic, lumbar, or sacral); (2) location and quantity of abscesses (unifocal, multifocal, discal, epidural, or paravertebral); (3) spinal cord compression, radicular compression; (4) cord signal changes (changing on both T1- and T2-weighted images). All the images were reviewed by a senior radiologist specialized in musculoskeletal imaging.

## Statistical analyses

Statistical analyses were performed using the Statistical Package for the Social Sciences software version 23.0 (IBM Corp., Armonk, NY). Continuous data were expressed as mean  $\pm$  standard deviation or median and interquartile range [M ( $P_{25}$ ,  $P_{75}$ )], while categorical data were expressed as the number of patients (percentage). Continuous data were compared between the two groups using the independent t-test or Mann–Whitney U test, while categorical data were compared using the Pearson  $\chi^2$  test or Fisher's exact test. Multi-factor analysis used binary logistic regression and screened independent variables by stepwise method. All statistical analyses were two-tailed and the significance level was set at P value  $< 0.05$ .

## Results

The clinical and laboratory data of the TS and PS groups were depicted in Table 1. Clinically, there was no significant difference in gender and course of disease between the TS and PS groups ( $p > 0.05$ ). The PS group had a significantly older age than the TS group ( $56 \pm 10$  years vs.  $49 \pm 15$  years,  $P = 0.005$ ). Based on the laboratory results, the PS group had a significantly greater WBC counts ( $6550 \pm 1960/\text{mm}^3$  vs.  $8690 \pm 3430/\text{mm}^3$ ,  $P < 0.000$ ), N counts ( $4710 \pm 1750/\text{mm}^3$  vs.  $6590 \pm 3190/\text{mm}^3$ ,  $P < 0.000$ ), L counts ( $1160 \pm 500/\text{mm}^3$  vs.  $1420 \pm 6100/\text{mm}^3$ ,  $P = 0.014$ ), ESR level ( $20 \pm 19$  mm/h vs.  $82 \pm 32$  mm/h,  $P < 0.000$ ) and CRP level ( $19.87 \pm 19.00$  mg/L vs.  $45.46 \pm 48.73$  mg/L,  $P = 0.001$ ). The FIB level of the function of blood coagulation was also significantly greater in the PS group than in the TS group ( $6.12 \pm 1.71$  g/L vs.  $4.67 \pm 1.27$  g/L,  $P < 0.001$ ). However, the serum A level ( $4.0 \pm 0.4$  g/dL vs.  $3.8 \pm 0.4$  g/dL,  $P = 0.005$ ) of the liver function tests and the serum Na level ( $141.6 \pm 3.1$  mmol/L vs.  $139.8 \pm 3.3$  mmol/L,  $P = 0.003$ ) of the serum electrolytes were significantly greater in the TS group than in the PS group.

The radiological characteristics of the TS and PS groups were summarized in Table 2. In the PS group, the proportions of cervical ( $n = 6$  [12.8%] vs.  $n = 1$  [1.5%],  $P = 0.043$ ) and lumbar ( $n = 35$  [74.5%] vs.  $n = 34$  [52.3%],  $P = 0.017$ ) vertebrae involved were higher than those in the TS group, while the proportions of thoracic ( $n = 13$  [27.7%] vs.  $n = 41$  [63.1%],  $P < 0.000$ ) vertebrae involved, epidural abscesses ( $n = 6$  [12.8%] vs.  $n = 23$  [35.4%],  $P = 0.007$ ), paravertebral abscesses ( $n = 18$  [38.3%] vs.  $n = 49$  [75.4%],  $P < 0.000$ ) and spinal cord compression ( $n = 9$  [19.1%] vs.  $n = 37$  [56.9%],  $P < 0.000$ ) were lower than those in the TS group.

The result of multivariate analysis by binary logistic regression were depicted in Table 3, and screened independent variables by stepwise method. Using this regression model proposed a diagnostic model that Y (value of TS  $> 0.5$ , value of PS  $< 0.5$ ) (Fig. 2) =  $1.251 * X1$  (thoracic vertebrae involved = 1, thoracic vertebrae uninvolved = 0) +  $2.021 * X2$  (paravertebral abscesses = 1, no paravertebral abscess = 0) +  $2.432 * X3$  (spinal cord compression = 1, no spinal cord compression = 0) +  $0.18 * X4$  (value of serum A) -  $4.209 * X5$  (cervical vertebrae involved = 1, cervical vertebrae uninvolved = 0) -  $0.02 * X6$  (value of ESR) -  $0.806 * X7$  (value of FIB) - 3.36.

The diagnostic model was tested with the original data, and the diagnostic value for TS and PS was presented in Table 4. Additionally, statistical measures of the diagnostic model's performance in diagnosing TS and PS were compared in Table 5. For the diagnosis of TS, the diagnostic model demonstrated 0.85 sensitivity, 0.85 specificity, 0.89 positive predictive value, 0.80 negative predictive value, and 0.85 accuracy. In the diagnosis of PS, the sensitivity, specificity, positive predictive value, negative predictive value, and accuracy were 0.85, 0.85, 0.80, 0.89, and 0.85, respectively. Furthermore, the model's performance was validated externally using a separate dataset, and the results were presented in Table 6. The diagnostic model's performance in diagnosing TS and PS in the external validation group was also described in Table 7. The diagnostic model achieved 0.84 sensitivity, 0.86 specificity, 0.88 positive predictive value, 0.82 negative predictive value, and 0.85 accuracy in diagnosing EV-TS, and 0.86 sensitivity, 0.84 specificity, 0.82 positive predictive value, 0.88 negative predictive value, and 0.85 accuracy in diagnosing EV-PS. These results suggest that the diagnostic model has significant potential in the diagnosis of both TS and PS.

## Discussion

Although there have been several previous studies<sup>8–10</sup> describing the characteristics of TS and PS, our comparative analysis of the two yields fifteen meaningful differentiating variables. However, no single diagnostic model is specific to either disease. Our diagnostic model is therefore a useful diagnostic tool that can help differentiate between TS and PS. A literature search reveals that our diagnostic model is the first of its kind for the differential diagnosis of TS and PS.

For laboratory findings, known risk factors for PS include greater levels of WBC counts, neutrophil counts, ESR and CRP<sup>8</sup>. Our study also found that L counts and FIB level might be valuable laboratory findings to diagnose spondylodiscitis. Elevated FIB levels often coincide with elevated acute-phase proteins, such as in bacterial infections like pneumonia, rheumatic fever, sepsis, etc. FIB interacts with inflammatory factors to affect the occurrence and development of diseases<sup>14,15</sup>. Univariate analyses indicated that greater levels of these biomarkers were suggestive of pyogenic rather than tuberculous spondylodiscitis. Meanwhile, greater levels of serum A and



|                               | Tuberculous group (n = 65) | Pyogenic group (n = 47) | t/ $\chi^2$ /Z Value | p Value |
|-------------------------------|----------------------------|-------------------------|----------------------|---------|
| Age (years)                   | 49 ± 15                    | 56 ± 10                 | − 2.874              | 0.005   |
| Men/Women                     | 37/28                      | 30/17                   | 0.541                | 0.462   |
| Course of disease (months)    | 6.0 (2.5, 12.0)            | 4.0 (2.0, 12.0)         | − 1.604              | 0.109   |
| Blood infection markers       |                            |                         |                      |         |
| WBC (/mm <sup>3</sup> )       | 6550 ± 1960                | 8690 ± 3430             | − 3.857              | < 0.000 |
| N (/mm <sup>3</sup> )         | 4710 ± 1750                | 6590 ± 3190             | − 3.667              | < 0.000 |
| E (/mm <sup>3</sup> )         | 140 ± 100                  | 120 ± 120               | 0.916                | 0.362   |
| B (/mm <sup>3</sup> )         | 30 ± 30                    | 30 ± 10                 | 0.814                | 0.417   |
| L (/mm <sup>3</sup> )         | 1160 ± 500                 | 1420 ± 610              | − 2.487              | 0.014   |
| M (/mm <sup>3</sup> )         | 520 ± 190                  | 530 ± 240               | − 0.343              | 0.732   |
| ESR (mm/h)                    | 20 ± 19                    | 82 ± 32                 | − 11.699             | < 0.000 |
| CRP (mg/L)                    | 19.87 ± 19.00              | 45.46 ± 48.73           | − 3.417              | 0.001   |
| Function of blood coagulation |                            |                         |                      |         |
| PLT (/mm <sup>3</sup> )       | 256,000 ± 64,000           | 290,000 ± 106,000       | − 1.977              | 0.052   |
| PT (s)                        | 12.2 ± 1.3                 | 12.5 ± 1.4              | − 1.088              | 0.279   |
| APTT (s)                      | 30.2 ± 5.5                 | 30.4 ± 5.7              | − 0.144              | 0.886   |
| TT (s)                        | 16.9 ± 0.9                 | 17.0 ± 1.1              | − 0.525              | 0.600   |
| FIB (g/L)                     | 4.67 ± 1.27                | 6.12 ± 1.71             | − 4.931              | < 0.000 |
| Kidney function tests         |                            |                         |                      |         |
| Cr (μmol/L)                   | 61.9 ± 16.2                | 59.1 ± 16.1             | 0.918                | 0.361   |
| GFR (mL/min)                  | 107.3 ± 19.2               | 105.9 ± 13.5            | 0.456                | 0.649   |
| Liver function tests          |                            |                         |                      |         |
| A (g/dL)                      | 4.0 ± 0.4                  | 3.7 ± 0.4               | 2.871                | 0.005   |
| G (g/dL)                      | 3.0 ± 0.4                  | 3.1 ± 0.7               | − 0.615              | 0.541   |
| ALT (U/L)                     | 28.1 ± 39.6                | 38.0 ± 36.9             | − 1.351              | 0.179   |
| AST (U/L)                     | 29.0 ± 29.8                | 28.5 ± 21.0             | 0.095                | 0.925   |
| Serum electrolytes            |                            |                         |                      |         |
| K (mmol/L)                    | 4.22 ± 0.53                | 4.17 ± 0.41             | 0.566                | 0.572   |
| Na (mmol/L)                   | 141.6 ± 3.1                | 139.8 ± 3.3             | 2.987                | 0.003   |
| Ca (mmol/L)                   | 2.25 ± 0.13                | 2.22 ± 0.12             | 1.139                | 0.257   |
| Cl (mmol/L)                   | 106.3 ± 3.5                | 105.1 ± 3.9             | 1.841                | 0.068   |

**Table 1.** Clinical data and laboratory examination of the tuberculous spondylitis group and pyogenic spondylodiscitis group. WBC indicates leukocyte; N, neutrophil; E, eosinophil; B, basophil; L, lymphocyte; M, monocyte; ESR, erythrocyte sedimentation rate; CRP, C-reactive protein; PLT, platelet; PT, prothrombin time; APTT, activated partial thromboplastin time; TT, prothrombin time; FIB, fibrinogen; Cr, creatinine; GFR, glomerular filtration rate; A, albumin; G, globulin; ALT, alanine transaminase; AST, aspartate transaminase; K, potassium; Na, potassium; Ca, calcium; Cl, chlorine. p-values derived from independent t-test, Pearson  $\chi^2$  test and Mann–Whitney U test.

Na were suggestive of tuberculous rather than pyogenic spondylodiscitis. However, the main function of serum Na is to maintain extracellular fluid volume, osmotic pressure and acid–base balance, and it also plays a role in maintaining normal muscle and nerve excitability.

Hematogenous spread accounts for more than 50% of spinal infections<sup>16</sup>. In most cases of TS and PS, pathogenic microorganisms remain near vertebral endplates, and then spread through the intervertebral discs to adjacent vertebral bodies and accessory structures. There is no blood supply in adult intervertebral discs<sup>17</sup>, and nutrition is contingent on diffusion from the endplates. When the endplates are damaged, the intervertebral space will narrow or possibly obliterate. Our study found no significant differences in the intervertebral disc spaces between TS and PS, but Galhotra<sup>18</sup> did. Lumbar segments are likely to be involved in PS, which could be due to their hematogenous spread, reflecting, to some extent, the vascular supply to lumbar structures<sup>19</sup>. This localization may also be related to the high mobility and load forces in the lumbar region<sup>20</sup>. In our study, 74.5% of PS patients had lumbar spine involvement (Fig. 3a and b) compared to 52.3% of TS patients and the difference was statistically significant. Thoracolumbar levels are commonly involved in TS, which may be explained by the coexistence of pulmonary tuberculosis as the origin of the hematogenous spread. In our study, 63.1% of TS patients had thoracic spine involvement (Fig. 3c and d), while this figure was only 27.7% in PS patients, and the difference was statistically significant.

In the abscesses, TS is more likely than PS to involve multiple segments with paravertebral spread and this is in agreement with our findings (Fig. 4). Previous studies<sup>21</sup> revealed that TS had a higher incidence rate of epidural abscess formation than PS. In our study, 35.4% of TS patients had epidural abscess formation compared

|                                    | Tuberculous group (n = 65) | Pyogenic group (n = 47) | t/ $\chi^2$ Value | p Value |
|------------------------------------|----------------------------|-------------------------|-------------------|---------|
| CT                                 |                            |                         |                   |         |
| Disc space narrowing               | 54 (83.1)                  | 33 (70.2)               | 2.603             | 0.107   |
| Bone destruction of vertebral body | 65 (100.0)                 | 47 (100.0)              | –                 | –       |
| Destruction of pedicle bone        | 11 (16.9)                  | 3 (6.4)                 | 2.771             | 0.096   |
| MRI                                |                            |                         |                   |         |
| Vertebral involvement              |                            |                         |                   |         |
| Single/Multiple-segment            | 3/62                       | 2/45                    | 0.000             | 1.000   |
| Cervical                           | 1 (1.5)                    | 6 (12.8)                | 4.108             | 0.043   |
| Thoracic                           | 41 (63.1)                  | 13 (27.7)               | 13.704            | <0.000  |
| Lumbar                             | 34 (52.3)                  | 35 (74.5)               | 5.663             | 0.017   |
| Sacral                             | 7 (10.8)                   | 7 (10.8)                | 0.424             | 0.515   |
| Abscesses                          |                            |                         |                   |         |
| Unifocal                           | 4 (6.2)                    | 6 (12.8)                | 0.766             | 0.381   |
| Multifocal                         | 52 (80.0)                  | 25 (53.2)               | 9.125             | 0.003   |
| Discal                             | 35 (53.8)                  | 25 (53.2)               | 0.005             | 0.945   |
| Epidural                           | 23 (35.4)                  | 6 (12.8)                | 7.273             | 0.007   |
| Paravertebral                      | 49 (75.4)                  | 18 (38.3)               | 15.609            | <0.000  |
| Spinal cord compression            | 37 (56.9)                  | 9 (19.1)                | 16.081            | <0.000  |
| Radicular compression              | 9 (13.8)                   | 3 (6.4)                 | 1.588             | 0.208   |
| Cord signal changes                | 4 (6.2)                    | 2 (4.3)                 | 0.000             | 0.988   |

**Table 2.** Imaging examination of the tuberculous spondylitis group and pyogenic spondylodiscitis group. p-values derived from Pearson  $\chi^2$  test and Fisher exact test.

| Variables               | Odds ratio | 95% confidence interval |        | p Value |
|-------------------------|------------|-------------------------|--------|---------|
| ESR                     | 0.980      | 0.958                   | 1.003  | 0.082   |
| FIB                     | 0.446      | 0.276                   | 0.723  | 0.001   |
| A                       | 1.197      | 1.014                   | 1.413  | 0.034   |
| Vertebral involvement   |            |                         |        |         |
| Cervical                | 0.015      | 0.000                   | 0.559  | 0.023   |
| Thoracic                | 3.495      | 0.994                   | 12.291 | 0.051   |
| Paravertebral abscesses | 7.543      | 1.962                   | 29.003 | 0.003   |
| Spinal cord compression | 11.382     | 2.494                   | 51.958 | 0.002   |

**Table 3.** Multivariate analysis of clinical, laboratory and radiological factors affecting diagnosis. ESR indicates erythrocyte sedimentation rate; FIB, fibrinogen; A, albumin. p-values derived from binary logistic regression.

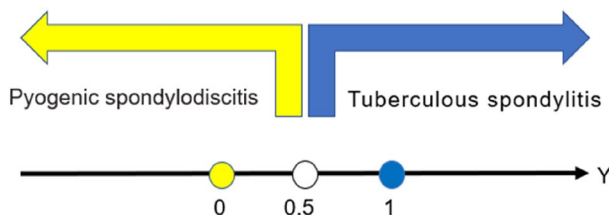


**Figure 2.** Diagnostic result corresponding to Y value.

with 12.8% of PS patients, while 37 TS patients (56.9%) and 9 PS patients (19.1%) presented with imaging signs of spinal cord compression, and both differences were statistically significant.

The above mentioned clinical characteristics are statistically significant and clinically correlated with the type of infection and can be used as efficient indicators for the differential diagnosis<sup>22,23</sup>. Logistic regression analysis is usually used as the model for differential diagnosis. In this study, we included three continuous variables and four categorical variables in the diagnostic model that yields great total accuracy for TS and PS diagnosis. However, there are limitations to our study. It is a retrospective study, with cases limited to a single Chinese institution.

| Diagnostic model | Pathology |    | Total |
|------------------|-----------|----|-------|
|                  | TS        | PS |       |
| TS               | 55        | 7  | 62    |
| PS               | 10        | 40 | 50    |
| Total            | 65        | 47 | 112   |

**Table 4.** The value of diagnostic model in the diagnosis of tuberculous spondylitis and pyogenic spondylodiscitis. TS indicates tuberculous spondylitis; PS, pyogenic spondylodiscitis.

| Disease | Se   | Sp   | PPV  | NPV  | Ac   |
|---------|------|------|------|------|------|
| TS      | 0.85 | 0.85 | 0.89 | 0.80 | 0.85 |
| PS      | 0.85 | 0.85 | 0.80 | 0.89 | 0.85 |

**Table 5.** Comparison of statistical indexes of the diagnostic model in the diagnosis of tuberculous spondylitis and pyogenic spondylodiscitis. TS indicates tuberculous spondylitis; PS, pyogenic spondylodiscitis; Se, sensitivity; Sp, specificity; PPV, positive predictive value; NPV, negative predictive value; Ac, accuracy.

| Diagnostic model | Pathology |    | Total |
|------------------|-----------|----|-------|
|                  | TS        | PS |       |
| TS               | 21        | 3  | 24    |
| PS               | 4         | 18 | 22    |
| Total            | 25        | 21 | 46    |

**Table 6.** External validation of the value of diagnostic model in the diagnosis of tuberculous spondylitis and pyogenic spondylodiscitis. TS indicates tuberculous spondylitis; PS, pyogenic spondylodiscitis.

| Disease | Se   | Sp   | PPV  | NPV  | Ac   |
|---------|------|------|------|------|------|
| TS      | 0.84 | 0.86 | 0.88 | 0.82 | 0.85 |
| PS      | 0.86 | 0.84 | 0.82 | 0.88 | 0.85 |

**Table 7.** The diagnostic performance of the diagnostic model in the external validation group of tuberculous spondylitis and pyogenic spondylodiscitis. TS indicates tuberculous spondylitis; PS, pyogenic spondylodiscitis; Se, sensitivity; Sp, specificity; PPV, positive predictive value; NPV, negative predictive value; Ac, accuracy.



**Figure 3.** CT scan images of tuberculous spondylitis and pyogenic spondylitis. (a and b) CT scan images of pyogenic spondylitis. Lumbar spine involvement is more common in pyogenic spondylitis. (c and d) CT scan images of tuberculous spondylitis. Thoracic spine involvement is more common in tuberculous spondylitis.

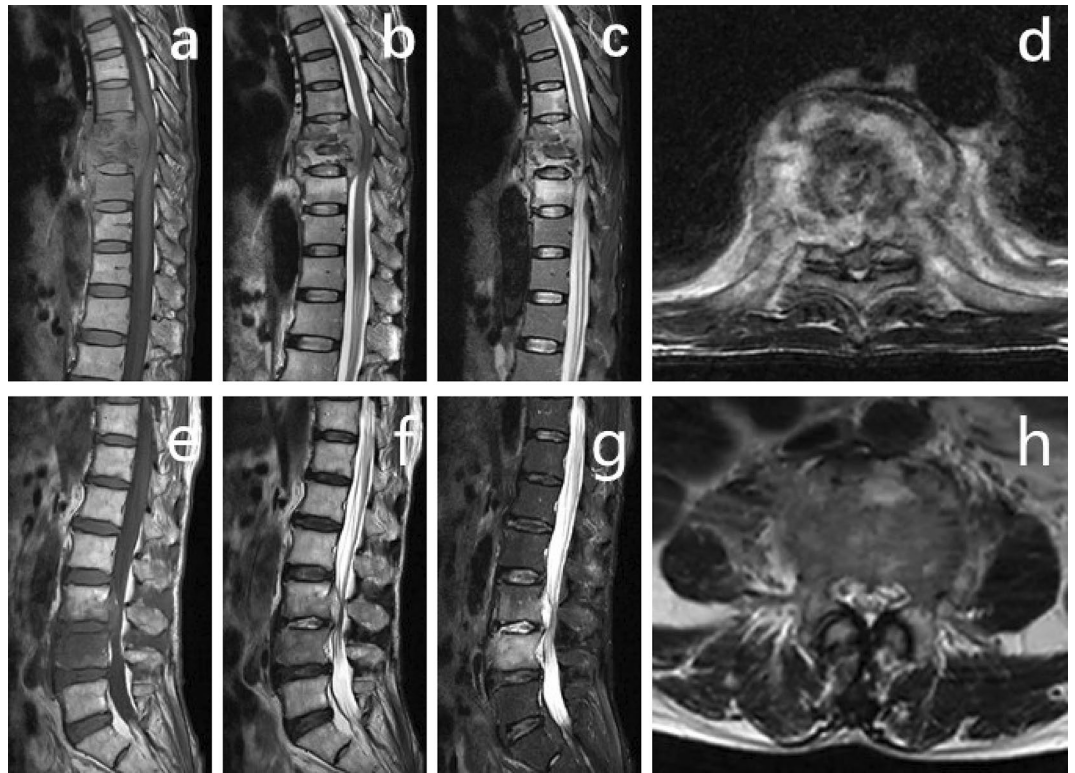


**Figure 4.** MRI scan images of tuberculous spondylitis and pyogenic spondylitis. (a–d) MRI scan images of tuberculous spondylitis. (e–h) MRI scan images of pyogenic spondylitis. In the abscesses, tuberculous spondylitis is more likely than pyogenic spondylitis to involve multiple segments with paravertebral spread.

Moreover, it is limited to inpatients with relatively advanced disease. Our diagnostic model is less useful early in the disease process, where many of the findings have not yet developed. In addition, the primary aim of this study was to construct a more widely applicable diagnostic model for clinical diagnosis and differential diagnosis of TS and PS by identifying differences in common laboratory and imaging examinations between the two. However, there were limitations in exploring their unknown differences.

## Conclusion

This study puts forward a diagnostic model for the diagnosis of TS and PS in spinal infection for the first time, which has potential guiding value in the diagnosis of them and provides a certain reference for clinical work.

## Data availability

All data generated or analysed during this study are included in this published article [and its supplementary information files].

Received: 22 November 2022; Accepted: 13 June 2023

Published online: 26 June 2023

## References

- Gouliouris, T., Aliyu, S. H. & Brown, N. M. Spondylodiscitis: Update on diagnosis and management. *J. Antimicrob. Chemother.* **65**, iii11–iii24. <https://doi.org/10.1093/jac/dkq303> (2010).
- Zhang, N. *et al.* The value of MR imaging in comparative analysis of spinal infection in adults: Pyogenic versus tuberculous. *World Neurosurg.* **128**, e806–e813. <https://doi.org/10.1016/j.wneu.2019.04.260> (2019).
- Doutchi, M. *et al.* Changing trends in the epidemiology of vertebral osteomyelitis in Marseille, France. *New Microbes New Infect.* **7**, 1–7. <https://doi.org/10.1016/j.nmni.2015.04.008> (2015).
- Skaf, G. S. *et al.* Pyogenic spondylodiscitis: An overview. *J. Infect. Public Health* **3**, 5–16. <https://doi.org/10.1016/j.jiph.2010.01.001> (2010).
- Jeong, S. J. *et al.* Microbiology and epidemiology of infectious spinal disease. *J. Korean Neurosurg. Soc.* **56**, 21–27. <https://doi.org/10.3340/jkns.2014.56.1.21> (2014).
- Sheikh, A. F. *et al.* pathogen identification in suspected cases of pyogenic spondylodiscitis. *Front. Cell Infect. Microbiol.* **7**, 60. <https://doi.org/10.3389/fcimb.2017.00060> (2017).
- Govender, S. Spinal infections. *J. Bone Joint Surg. Am.* **87**, 1454–1458. <https://doi.org/10.1302/0301-620X.87B11> (2005).
- Yoon, Y. K. *et al.* Differential diagnosis between tuberculous spondylodiscitis and pyogenic spontaneous spondylodiscitis: A multicenter descriptive and comparative study. *Spine J.* **15**, 1764–1771. <https://doi.org/10.1016/j.spinee.2015.04.006> (2015).

9. Naselli, N. *et al.* MRI in differential diagnosis between tuberculous and pyogenic spondylodiscitis. *Eur. Spine J.* **31**, 431–441. <https://doi.org/10.1007/s00586-021-06952-8> (2022).
10. Liu, X., Zheng, M., Sun, J. & Cui, X. A diagnostic model for differentiating tuberculous spondylitis from pyogenic spondylitis on computed tomography images. *Eur. Radiol.* **31**, 7626–7636. <https://doi.org/10.1007/s00330-021-07812-1> (2021).
11. Gregori, F. *et al.* Treatment algorithm for spontaneous spinal infections: A review of the literature. *J. Craniovertebr. Junct. Spine* **10**, 3–9. [https://doi.org/10.4103/jcvjs.JCVJS\\_115\\_18](https://doi.org/10.4103/jcvjs.JCVJS_115_18) (2019).
12. Gemmel, F. *et al.* Multimodality SPECT imaging of multifocal spondylodiscitis. *Clin. Nucl. Med.* **29**, 635–636. <https://doi.org/10.1097/00003072-200410000-00009> (2004).
13. Stumpe, K. D. M. *et al.* FDG positron emission tomography for differentiation of degenerative and infectious endplate abnormalities in the lumbar spine detected on MR imaging. *AJR Am. J. Roentgenol.* **179**, 258. <https://doi.org/10.2214/ajr.179.5.1791151> (2002).
14. Hoppe, B. Fibrinogen and factor XIII at the intersection of coagulation, fibrinolysis and inflammation. *Thromb. Haemost.* **112**, 649–658. <https://doi.org/10.1160/TH14-01-0085> (2014).
15. Hsieh, J. Y. *et al.* Differential regulation of macrophage inflammatory activation by fibrin and fibrinogen. *Acta Biomater.* **47**, 14–24. <https://doi.org/10.1016/j.actbio.2016.09.024> (2017).
16. Tali, E. T., Oner, A. Y. & Koc, A. M. Pyogenic spinal infections. *Neuroimaging Clin. N. Am.* **25**, 193–208. <https://doi.org/10.1016/j.nic.2015.01.003> (2015).
17. Babic, M. & Simpfendorfer, C. S. Infections of the Spine. *Infect. Dis. Clin. N. Am.* **31**, 279–297. <https://doi.org/10.1016/j.idc.2017.01.003> (2017).
18. Galhotra, R. D., Jain, T., Sandhu, P. & Galhotra, V. Utility of magnetic resonance imaging in the differential diagnosis of tubercular and pyogenic spondylodiscitis. *J. Nat. Sci. Biol. Med.* **6**, 388–393. <https://doi.org/10.4103/0976-9668.160016> (2015).
19. Pigrau-Serrallach, C. & Rodriguez-Pardo, D. Bone and joint tuberculosis. *Eur. Spine J.* **22**(Suppl 4), 556–566. <https://doi.org/10.1007/s00586-012-2331-y> (2013).
20. Ozaksoy, D. *et al.* Brucellar spondylitis: MRI findings. *Eur. Spine J.* **10**, 529–533. <https://doi.org/10.1007/s005860100285> (2001).
21. Harada, Y., Tokuda, O. & Matsunaga, N. Magnetic resonance imaging characteristics of tuberculous spondylitis vs. pyogenic spondylitis. *Clin. Imaging* **32**, 303–309. <https://doi.org/10.1016/j.clinimag.2007.03.015> (2008).
22. Yang, Z., Feng, L., Huang, Y. & Xia, N. A differential diagnosis model for diabetic nephropathy and non-diabetic renal disease in patients with type 2 diabetes complicated with chronic kidney disease. *Diabetes Metab. Syndr. Obes.* **12**, 1963–1972. <https://doi.org/10.2147/DMSO.S223144> (2019).
23. Wang, L. W. *et al.* Establishing a model to measure and predict the quality of gastrointestinal endoscopy. *World J. Gastroenterol.* **25**, 1024–1030. <https://doi.org/10.3748/wjg.v25.i8.1024> (2019).

## Acknowledgements

Finally, we would like to express our gratitude to Dr. Xiaolan Feng, the radiologist, and Dr. Xingwang Sun, the pathologist, for their significant help and support in this study. Their professional knowledge and skills were crucial to the smooth completion of this paper, and we sincerely thank them for their hard work and selfless dedication.

## Author contributions

The study was designed by Y.X.L. and D.X.F. Data acquisition and data analysis was performed by Y.X.L. Data interpretation was performed by Y.X.L., F.L. and D.X.F. The manuscript was drafted by Y.X.L. The manuscript was revised by F.L., L.P.Z., H.Y., Q.Z.Z. and D.X.F. All authors read and approved the final manuscript.

## Competing interests

The authors declare no competing interests.

## Additional information

**Supplementary Information** The online version contains supplementary material available at <https://doi.org/10.1038/s41598-023-36965-w>.

**Correspondence** and requests for materials should be addressed to D.X.F.

**Reprints and permissions information** is available at [www.nature.com/reprints](http://www.nature.com/reprints).

**Publisher's note** Springer Nature remains neutral with regard to jurisdictional claims in published maps and institutional affiliations.



**Open Access** This article is licensed under a Creative Commons Attribution 4.0 International License, which permits use, sharing, adaptation, distribution and reproduction in any medium or format, as long as you give appropriate credit to the original author(s) and the source, provide a link to the Creative Commons licence, and indicate if changes were made. The images or other third party material in this article are included in the article's Creative Commons licence, unless indicated otherwise in a credit line to the material. If material is not included in the article's Creative Commons licence and your intended use is not permitted by statutory regulation or exceeds the permitted use, you will need to obtain permission directly from the copyright holder. To view a copy of this licence, visit <http://creativecommons.org/licenses/by/4.0/>.

© The Author(s) 2023